Simulation of laser wakefield acceleration of an ultrashort electron bunch

A. J. W. Reitsma,[1] V. V. Goloviznin,[1] L. P. J. Kamp,[1] and T. J. Schep[2]
[1]*Technische Universiteit Eindhoven, P.O. Box 513, 5600 MB Eindhoven, The Netherlands*
[2]*FOM Instituut voor Plasmafysica Rijnhuizen, P.O. Box 1207, 3430 BE Nieuwegein, The Netherlands*
(Received 27 June 2000; published 29 March 2001)

The dynamics of the acceleration of a short electron bunch in a strong plasma wave excited by a laser pulse in a plasma channel is studied both analytically and numerically in slab geometry. In our simulations, a fully nonlinear, relativistic hydrodynamic description for the plasma wave is combined with particle-in-cell methods for the description of the bunch. Collective self-interactions within the bunch are fully taken into account. The existence of adiabatic invariants of motion is shown to have important implications for the final beam quality. Similar to the one-dimensional case, the natural evolution of the bunch is shown to lead, under proper initial conditions, to a minimum in the relative energy spread.

DOI: 10.1103/PhysRevE.63.046502 PACS number(s): 29.27.Fh, 41.75.Jv, 52.40.Mj, 52.75.Di

I. INTRODUCTION

The study of plasma-based devices for acceleration of electron beams has gained a lot of interest lately, in particular because recent advances in laser technology have made it possible to produce ultrashort, ultraintense pulses, which can drive high-amplitude plasma waves (wakefields) in a plasma [1–3].

The maximal acceleration length in one acceleration section is determined by phase slippage. Ideally, one would like to use the full dephasing length for acceleration, but due to diffraction, the acceleration length in a homogeneous plasma cannot exceed the Rayleigh length, which is usually orders of magnitude smaller. Therefore, in order to take full advantage of the extremely high accelerating gradients of order 10–100 GeV/m that occur in plasma-based acceleration, one needs to form a guiding structure for the laser pulse [4].

The plasma channel as a guiding structure is currently under active investigation [5–10]. In a plasma channel, the on-axis density depression acts as an optical fiber by changing locally the value of the refractive index. It has been shown [11,12] that for a hollow channel with a ''square'' density profile, the wakefield has optimal properties in conserving the beam quality of accelerated electrons. A more realistic approach would involve a smooth density distribution. The accelerating properties of laser wakefields in smooth density channels are discussed in Refs. [13–15].

The energy acquired by an electron by acceleration in a plasma wave depends on the injection phase [16,17]. To minimize energy spread, a phasing strategy for one-dimensional acceleration has been proposed earlier [22,23]. In this paper, we discuss the generalization of this scheme to the case of a two-dimensional setting, including the effects of transverse motion on beam quality.

Due to the short plasma wavelength, phase control is a severe problem. Controlled acceleration is possible for short bunches of preaccelerated electrons, either by direct injection from an rf gun [18] or by optical injection with laser pulses [19–21]. The production of such short bunches is a major challenge for the realization of controlled LWFA: production of bunches with sub-ps length has been reported [24], but in this case the required (low) energy spread is lacking. To the best of our knowledge, no experiment has yet produced a (sub-) 100 fs bunch with sufficiently small energy spread. However, at Eindhoven University of Technology, a photocathode rf electron gun based on sophisticated techniques is currently under development [25]: numerical modeling predicts the possibility of producing 1 nC, 100 fs electron bunches with less than a few percent energy spread.

This paper is organized as follows. In Sec. II, the structure of the wakefield is described using nonlinear hydrodynamic equations. In Sec. III, we present analytical results on electron acceleration in wakefields. In Sec. IV, the acceleration process is studied numerically. Section V is devoted to summary and conclusions.

II. WAKEFIELD DESCRIPTION

As mentioned before, we consider a channel-guided laser wakefield acceleration scheme. The performed plasma channel is assumed to have a stationary density profile that depends only on the transverse coordinate. To be specific, we use the following expression:

$$n_0(x) = n_{00}[1 - \Delta(1 - x^2/W^2)e^{-x^2/2W^2}],$$

where n_{00} is the ambient plasma density, x is the transverse coordinate, Δ is the density modulation, and W is the channel width. This form of plasma channel is close to what has been found in recent experiments [26,27]. As an example, a density profile with $\Delta = 0.5$ is given in Fig. 1.

The excited wakefield is described by a set of fully nonlinear hydrodynamic equations [28,29] for the motion of plasma electrons (plasma ions are taken to be immobile). The quasistatic approximation is applied, so that all fields depend on the longitudinal coordinate z and time t only through the combination $\zeta = z - v_\varphi t$, where v_φ is the group velocity of the laser pulse. The corresponding Lorentz factor γ_φ is taken to be large ($\gamma_\varphi \gg 1$), so that in calculating the wakefields v_φ may be approximated with c [30].

The ponderomotive potential I of the laser pulse is considered to be a given function of x and ζ:

$$I = I_0 f_1(\zeta) f_2(x),$$

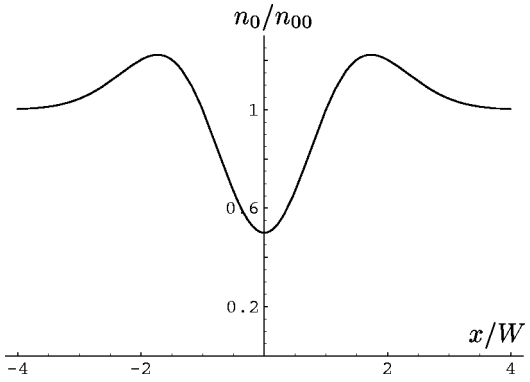

FIG. 1. Density profile with $\Delta = 0.5$.

where I_0 denotes the maximal intensity. The axial profile is chosen to be

$$f_1(\zeta) = \begin{cases} \left[1 - \left(\dfrac{\zeta - \zeta_0}{L}\right)^2\right]^3, & |\zeta - \zeta_0| < L \\ 0, & |\zeta - \zeta_0| \geqslant L, \end{cases}$$

where ζ_0 is the position of the laser pulse and $0.908L$ its full width at half maximum (FWHM). The radial profile is Gaussian,

$$f_2(x) = e^{-x^2/R^2},$$

where R is the width of the laser pulse. For R, we take the value that gives matched propagation (i.e., without oscillations in size or amplitude) in a parabolic channel [31,32]:

$$R = \left(\frac{2}{3\Delta}\right)^{1/4} W^{1/2}.$$

In Fig. 2, a plot of the ponderomotive potential is given.

We introduce the following dimensionless quantities: time $\tilde{t} = \omega_p t$, coordinates $(\tilde{x}, \tilde{z}) = k_p(x,z)$, ion (background) density $\tilde{n}_0 = n_0/n_{00}$, plasma electron density $\tilde{n} = n_e/n_{00}$, bunch electron density $\tilde{n}_b = n_b/n_{00}$, plasma electron momentum $(\tilde{p}_x, \tilde{p}_z) = (p_x, p_z)/(m_e c)$, plasma electron velocity $(\tilde{v}_x, \tilde{v}_z) = (v_x, v_z)/c$, and wakefield components $(\tilde{E}_x, \tilde{B}_y, \tilde{E}_z) = e(E_x, B_y, E_z)/(m_e \omega_p c)$. In what follows, the tildes are dropped for convenience. Here ω_p and k_p are the electron plasma frequency and the wave number associated with the ambient plasma density n_{00}: $\omega_p^2 = 4\pi n_{00} e^2/m_e$, $k_p = \omega_p/c$.

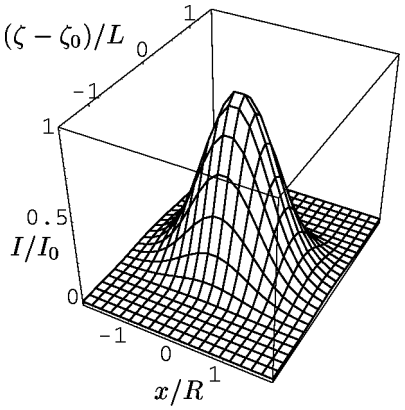

FIG. 2. Laser profile $I(x,\zeta)$.

As usual, the (averaged) Lorentz factor of plasma electrons is defined as $\gamma_p = \sqrt{1 + p_x^2 + p_z^2 + 2I}$ and the wakefield potential $\Phi = \gamma_p - p_z$ such that

$$F_x = -E_x + B_y = \frac{\partial \Phi}{\partial x},$$

$$F_z = -E_z = \frac{\partial \Phi}{\partial \zeta},$$

where F_x, F_z denote components of the Lorentz force acting on an ultrarelativistic (bunch) electron. The wakefield equations are combined to (see the Appendix)

$$\frac{\partial^2 \Phi}{\partial \zeta^2} - \frac{\partial^2 \Phi}{\partial x^2} - \frac{\partial^2}{\partial x \partial \zeta}\left(\frac{1}{\eta}\frac{\partial^2 \Phi}{\partial x \partial \zeta}\right) + \eta \Phi = \eta \gamma_p - \frac{\partial^2 \gamma_p}{\partial x^2} + n_b, \tag{1}$$

where we introduce the quantity $\eta = n/\gamma_p$. Equation (1) is highly nonlinear through the dependence of γ_p and η on Φ:

$$\eta = \frac{1}{\Phi}\left(n_0 + \frac{\partial^2 \Phi}{\partial x^2}\right),$$

$$\gamma_p = \frac{1}{2\Phi}\left[1 + \Phi^2 + \left(\frac{1}{\eta}\frac{\partial^2 \Phi}{\partial x \partial \zeta}\right)^2 + 2I\right].$$

The above equations are solved numerically under the conditions that the plasma is at rest ahead of the laser pulse ($\Phi = 1$ for $\zeta \geqslant 0$) and that the fields fall off exponentially at large $|x|$. A typical field and density distribution is given in Fig. 3, which shows contour plots of η, Φ, F_x, F_z, B_y, and a combined plot of I and n_b. The parameters are (in dimensionless units) channel width $W = 3.141$, channel modulation $\Delta = 0.5$, laser spot size $R = 1.905$, laser pulse length $L = 1.111$, and peak amplitude $I_0 = 0.2$. The electron bunch parameters are length $\delta\zeta = 0.47$, width $\delta x = 0.47$, normalized transverse emittance $\sigma_x = 0.022$, and peak of n_b (electron bunch density) 0.143. In dimensional units, these numbers correspond to a bunch of width and length 40 fs or 11.8 μm FWHM, normalized transverse emittance 0.35 mm mrad, and a peak current of about 0.1 kA for a plasma wavelength of $\lambda_p = 100$ μm.

In Fig. 3, it can be seen that the amplitude of the focusing force increases with the distance behind the pulse and the amplitude of the accelerating force decreases with the distance behind the pulse. The overlap of focusing and accelerating regions behind the laser pulse is clearly visible. These features are in accordance with the results of Ref. [13]. Also visible in Fig. 3 is the influence of the electron bunch, on the wakefields, caused by *beam loading*. Inside and directly behind the bunch there is enhanced focusing and diminished

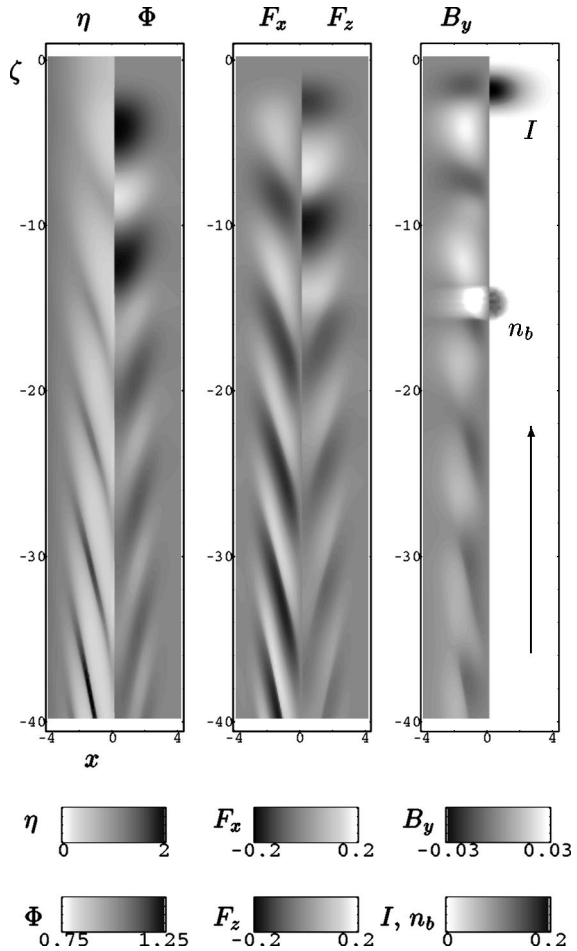

FIG. 3. Contour plots of η, Φ, F_x, F_z, B_y, I and n_b as functions of x, ζ. The arrow indicates the direction of propagation.

acceleration. The magnetic field around the bunch is strong, even outside the given range. The cutoff was used in order not to spoil the fine details of the field structure behind the bunch. The plot of η exhibits narrow regions with high plasma-electron density, corresponding to sharp gradients in F_x, F_z.

III. RELATIVISTIC ELECTRON DYNAMICS IN A WAKEFIELD

In this section, we first discuss the acceleration process on the one-particle level and later include effects due to finite width and length of the bunch as well as beam loading.

A. Motion of a single electron

The Hamiltonian for a relativistic electron in a wakefield is

$$H=\gamma-v_\varphi P_z-\Phi,$$

where $\gamma=\sqrt{1+P_z^2+P_x^2}$ is the electron's Lorentz factor and $\vec{P}=(P_x,P_z)$ its (dimensionless) momentum. In the small-angle approximation, the Hamiltonian can be split into longitudinal and transverse parts: $H\approx H_\parallel+H_\perp$. The longitudinal part is identical to the Hamiltonian of an electron in a one-dimensional wakefield:

$$H_\parallel=\gamma_\parallel-v_\varphi P_z-\Phi^{(0)},$$

where $\gamma_\parallel=\sqrt{1+P_z^2}$ and the superscript means taking the on-axis value, so that $\Phi^{(0)}\equiv\Phi(\zeta,x=0)$ is a function of ζ only. The one-dimensional equations of motion are

$$\frac{d\zeta}{dt}=\frac{P_z}{\gamma_\parallel}-v_\varphi, \tag{2}$$

$$\frac{dP_z}{dt}=\Phi_\zeta^{(0)}, \tag{3}$$

where the subscript denotes a corresponding derivative of Φ. The first equation describes phase slippage and the second the energy transfer between the electron and the wakefield. For large energies $\gamma_\parallel\gg\gamma_\varphi$ we can approximately solve the phase-slippage equation:

$$\frac{d\zeta}{dt}\approx\frac{1}{2\gamma_\varphi^2}. \tag{4}$$

From this we can estimate a typical time scale (in dimensionless units) for longitudinal motion as

$$\tau_\parallel\simeq\gamma_\varphi^2.$$

The transverse part of the Hamiltonian is

$$H_\perp=\frac{1}{2}\left(\frac{P_x^2}{\gamma_\parallel}-\Phi_{xx}^{(0)}x^2\right),$$

where $\Phi_{xx}^{(0)}$ denotes the curvature of the potential Φ in the vicinity of the axis. For $\Phi_{xx}^{(0)}<0$, $H_\perp$ is the Hamiltonian of a harmonic oscillator that depends on the variables ζ and P_z as parameters. We can take the (ζ,P_z) dependence to be adiabatically slow if the time scale involved in transverse oscillation is much shorter than the time scale of longitudinal motion. In that case, the time scale of a transverse oscillation can be estimated as

$$\tau_\perp\simeq\gamma_\parallel^{1/2}|\Phi_{xx}^{(0)}|^{-1/2}.$$

One can easily see that the condition $\tau_\perp/\tau_\parallel\ll1$ is satisfied for a large part of the acceleration process unless the particle's energy is extremely high (of order 100 TeV for $\gamma_\varphi=100$) or the electron slips too close to a defocusing region (i.e., near a point where $\Phi_{xx}^{(0)}=0$).

The existence of adiabatic invariance for the transverse motion means the conservation of the area enclosed in transverse phase space,

$$\oint P_x dx=\text{const}.$$

Thus the product of x_0 and P_0, the amplitudes of oscillation of x and P_x, is a constant:

$$x_0 P_0 = A_0 .$$

Combining this with the equations of motion results in

$$x_0 = A_0^{1/2} \gamma_\parallel^{-1/4} |\Phi_{xx}^{(0)}|^{-1/4}. \tag{5}$$

If an electron remains inside the focusing region, $\Phi_{xx}^{(0)}$ will change only slightly, but the electron's $\gamma_\parallel$ may go up from about 10 to about 3000. In that case, Eq. (5) indicates that the amplitude of the transverse oscillation goes down rapidly by a factor of about 4. This focusing effect of the accelerated electrons, which occurs as a consequence of adiabatic invariance, is observed clearly in our simulation results (see Sec. IV).

The focusing of an accelerated electron has an important implication for the energy spread. The averaged equation for energy gain is

$$\frac{dP_z}{dt} = \Phi_\zeta^{(0)} + \frac{1}{2}\Phi_{\zeta xx}^{(0)} \widehat{x^2}, \tag{6}$$

where the caret denotes averaging over the transverse oscillations. Equation (6) describes the first-order correction to Eq. (3) due to transverse motion by taking into account transverse variations of the accelerating field. Since commonly $\Phi_{\zeta xx}^{(0)} < 0$, it was concluded that electrons undergoing large transverse oscillations gain less energy than electrons close to the axis [33–35]. However, this is not always true. As mentioned before, due to focusing, the value of $\widehat{x^2}$ decreases and the influence of the $\widehat{x^2}$-term becomes less important as the electron gains energy. To fully appreciate the effects of transverse oscillations we must also consider its effect on phase slippage, given by

$$\frac{d\zeta}{dt} = \frac{P_z}{\gamma_\parallel}\left(1 - \frac{\widehat{P_x^2}}{2\gamma_\parallel^2}\right) - v_\varphi . \tag{7}$$

This equation describes the first-order correction to Eq. (2) due to transverse motion. For electrons at $\gamma_\parallel \gg \gamma_\varphi$, this correction is very small and can be neglected. For electrons injected at $\gamma_\parallel < \gamma_\varphi$, as considered here, the effect must be taken into account and leads to a phase difference for particles with different amplitudes of transverse oscillation. If this phase difference is large enough, it is the longitudinal rather than transverse variations in an accelerating field that determine the energy difference between particles with different amplitudes of oscillation.

B. Bunch effects

An important issue is the effect of finite width on transverse emittance. Due to adiabatic invariance, the area enclosed in transverse phase space is conserved for each individual trajectory. From this we conclude that the transverse emittance is conserved insofar as the bunch distribution is *matched* to the phase-space orbits of the transverse Hamiltonian [36]. For mismatched beams, nonlinearities in the focusing force will cause emittance growth in the first part of the acceleration. Since the transverse motion is much faster than the longitudinal one, we may consider the phase-space orbits corresponding to the initial values of $\gamma_\parallel$ and $\Phi_{xx}^{(0)}$. Examples of matched and mismatched distributions are given in Fig. 4.

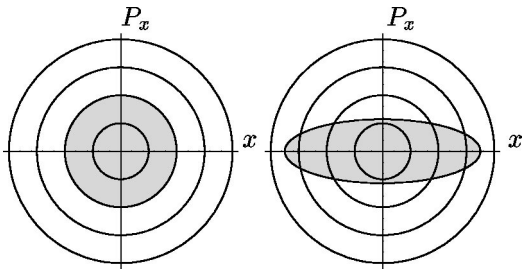

FIG. 4. Matched (left) and mismatched (right) initial bunch distributions: circles are phase space orbits, gray area represents particle distribution of the electron bunch.

Note that the effect of beam loading on transverse emittance is relatively unimportant. The bunch wakefields introduce extra focusing in the rear part of the bunch, which leads to a change in $\Phi_{xx}^{(0)}$. The bunch adjusts itself to the potential on the short time scale $\tau_\perp$, whereas the evolution of bunch wakefields takes place on the long time scale $\tau_\parallel$ of longitudinal motion. Consequently, the adiabatic invariance is not influenced by collective effects and there is no additional emittance growth. By a similar reasoning, one finds that the effects of finite bunch length on transverse emittance are unimportant.

Now let us discuss the effect of finite bunch length on energy spread. Since $\gamma_\parallel \gg \gamma_\varphi$ holds for a large part of the acceleration, we may use the approximate solution for phase slippage [Eq. (4)] to determine energy gain ΔP_z for a particle injected at $\zeta_{\rm in}$ and extracted at $\zeta_{\rm ex}$:

$$\Delta P_z = 2\gamma_\varphi^2 [\Phi^{(0)}(\zeta_{\rm ex}) - \Phi^{(0)}(\zeta_{\rm in})]. \tag{8}$$

For a short bunch injected with typical phase spread $\delta\zeta \ll \lambda_p$ around the injection phase, we may estimate the cumulative energy spread $\delta P_z^{(1)}$ from Eq. (8) as

$$\delta P_z^{(1)} = 2\gamma_\varphi^2 \delta\zeta [\Phi_\zeta^{(0)}(\zeta_{\rm ex}) - \Phi_\zeta^{(0)}(\zeta_{\rm in})]. \tag{9}$$

This equation suggests that there are two strategies to minimize energy spread: either use a very short bunch to minimize $\delta\zeta$ [37] or arrange injection and extraction phases such that

$$\Phi_\zeta^{(0)}(\zeta_{\rm ex}) - \Phi_\zeta^{(0)}(\zeta_{\rm in}) = 0.$$

Note that this can also be written as

$$(\zeta_{\rm ex} - \zeta_{\rm in})\Phi_{\zeta\zeta}^{(0)}(\zeta_M) = 0,$$

where ζ_M denotes a certain point in the interval $[\zeta_{\rm in}, \zeta_{\rm ex}]$. Therefore, this minimizing strategy requires that the accelerating gradient has its maximum somewhere between $\zeta_{\rm in}$ and $\zeta_{\rm ex}$. At the same time, the transverse stability requires that the particles remain inside the focusing region. For two-dimensional wakefields in a homogeneous plasma, the above conditions cannot be satisfied simultaneously, since typically

the accelerating gradient has its maximum at the edge of the focusing region. However, the overlap of focusing and accelerating regions is the unique feature for wakefields in plasma channels that makes it possible to apply the second minimizing strategy.

The effect of beam loading on energy spread is determined by the modification of the accelerating force inside the bunch due its own wakefields. The cumulative energy difference $\delta P_z^{(2)}$ due to beam loading can be estimated as

$$\delta P_z^{(2)} = 2\chi\gamma_\varphi^2(\zeta_{\rm ex}-\zeta_{\rm in}), \tag{10}$$

where χ denotes the beam-loading efficiency. Generally speaking, 100% beam loading corresponds to the maximal charge that can be accelerated. As a rather simple definition we use

$$\chi = \alpha\frac{Q}{I_0},$$

where

$$Q = \int n_b(x,\zeta)dx\,d\zeta$$

is the total charge in the bunch. The coefficient $\alpha \approx 0.33$ is determined empirically from comparing on-axis amplitudes of wakefields excited by the laser pulse and the electron bunch separately. The condition for minimum energy spread is that the terms in Eq. (9) and Eq. (10) cancel each other:

$$\delta\zeta[\Phi_\zeta^{(0)}(\zeta_{\rm ex})-\Phi_\zeta^{(0)}(\zeta_{\rm in})]+\chi(\zeta_{\rm ex}-\zeta_{\rm in})=0. \tag{11}$$

This condition can be satisfied if a point ζ_M in the interval $[\zeta_{\rm in},\zeta_{\rm ex}]$ exists such that

$$\Phi_{\zeta\zeta}^{(0)}(\zeta_M) = -\frac{\chi}{\delta\zeta}.$$

The above condition was derived for one-dimensional acceleration [22,23], but it appears to be applicable in the two-dimensional case as well.

IV. SIMULATION RESULTS

To study the bunch dynamics self-consistently, a numerical integration of the equations of motion

$$\frac{dx}{dt} = v_x,$$

$$\frac{d\zeta}{dt} = v_z - v_\varphi,$$

$$\frac{dP_x}{dt} = F_x,$$

$$\frac{dP_z}{dt} = F_z$$

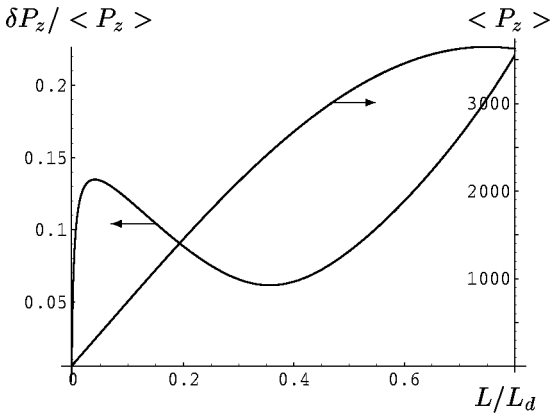

FIG. 5. Energy and relative energy spread as functions of acceleration length L/L_d.

has been performed. As mentioned before, the bunch density as a source term is included in the calculation of F_x, F_z. This permits a study of the influence of beam loading on the acceleration process.

In Figs. 5 and 6, the results of a simulation with beam loading $\chi = 0.17$ and $\gamma_\varphi = 100$ are shown. The electron bunch is injected at $\zeta_{\rm in} = -14.92$, with energy $\langle P_z\rangle = 20$ (where $\langle\cdots\rangle$ denotes averaging over the bunch distribution), spatial dimensions $\delta\zeta = 0.47$, $\delta x = 0.15$, and normalized rms transverse emittance $\sigma_x = 0.022$. These parameters correspond to the bunch depicted in Fig. 3, except that δx is smaller.

In Fig. 5, the energy gain and relative energy spread are shown as functions of acceleration length, given as a fraction of the dephasing length $L_d = \gamma_\varphi^2\lambda_p$. A minimum in energy spread of about 6.5% is seen to occur after accelerating over a length $L = 0.39L_d$. At this point, $\langle P_z\rangle$ is 2750 (1.4 GeV).

In Fig. 6, a few snapshots of (ζ, P_z)-phase space are depicted. It is clearly seen that the ''thickness'' of the distribution (energy spread at a given phase) is small compared to the total energy spread. From this we conclude that the finite length of the bunch is a much more important source for energy spread than finite width. Also clearly visible is the cancellation effect of energy spread: in the first stage of acceleration, the front of the bunch gains more energy than the rear; in the second stage, the rear gains more than the front.

In Fig. 7, transverse emittance as a function of accelera-

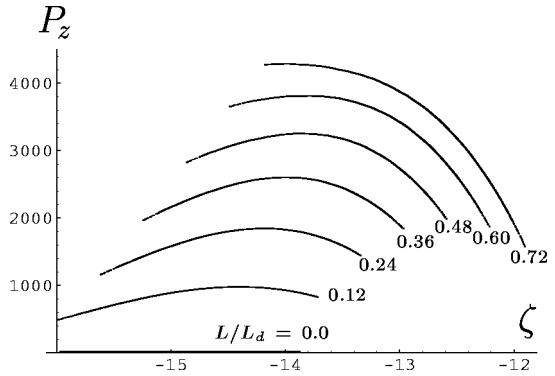

FIG. 6. Phase-space snapshots at various acceleration lengths L/L_d.

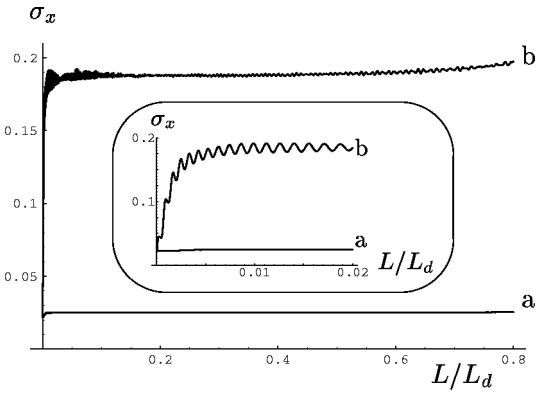

FIG. 7. Transverse emittance as a function of acceleration length L/L_d (inset: detail).

tion length is shown for a matched bunch and for a mismatched bunch. The matched bunch has the same parameters as the one in Figs. 5 and 6. The mismatched bunch has the same initial conditions, except that it is wider (namely, $\delta x = 0.47$, corresponding to Fig. 3). Figure 7 clearly shows emittance conservation for both bunches during a large part of the acceleration. In the inset, a detail of the beginning of the acceleration is given, which shows rapid emittance growth for the mismatched bunch.

For these bunches, a plot of δx and $\delta\zeta$ as functions of acceleration length is shown in Fig. 8. This plot shows a rapid focusing of the bunches, accompanied by a slight increase in bunch length. These effects are more pronounced for the mismatched bunch.

V. SUMMARY AND CONCLUSIONS

In summary, we have studied the dynamics of an accelerated electron bunch in a channel-guided laser wakefield accelerator in a plasma channel, paying particular attention to beam quality. We have analyzed the influence of transverse bunch dynamics on transverse emittance and energy spread. Due to the difference in time scales of longitudinal and transverse motion, there exists an adiabatic invariant for the transverse motion. This invariance results in conservation of transverse emittance for matched beams, even with beam-loading effects taken into account. As for relative energy spread, we have shown that the strategy of optimal phasing developed in [22] for one-dimensional acceleration can be successfully applied to our two-dimensional setting as well. The main reason for this is the transverse focusing of the electron bunch, which strongly reduces the influence of transverse dynamics on the final energy spread. Under proper initial conditions we find that the main contributions to the energy spread, namely due to finite bunch length [Eq. (9)] and beam loading [Eq. (10)], may cancel each other, resulting in a low relative energy spread.

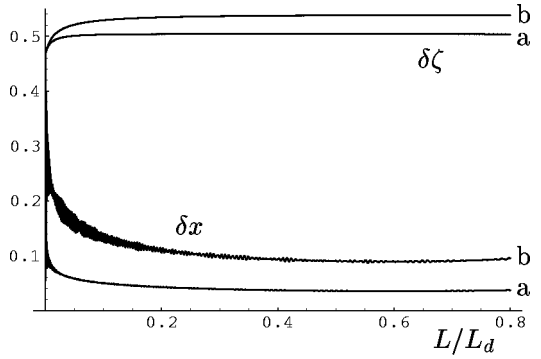

FIG. 8. Bunch width δx and bunch length $\delta\zeta$ as functions of acceleration length L/L_d for matched (a) and mismatched (b) bunch.

APPENDIX: NONLINEAR WAKEFIELD EQUATIONS

Using Faraday's equation, it is easy to show that the relation

$$\vec{B} = \vec{\nabla} \times \vec{p}$$

holds for all $t>0$ if it holds at $t=0$, as a consequence of conservation of the flux of generalized vorticity. From the momentum balance, an expression for the electric field is derived:

$$\vec{E} = -\frac{\partial \vec{p}}{\partial t} - \vec{\nabla}\gamma_p ,$$

where

$$\gamma_p = \sqrt{1+\vec{p}^2+2I}$$

is the Lorentz factor of plasma electrons, averaged over the ''fast'' oscillations in the optical field. Combining the above relations with Ampère's law yields

$$\frac{\partial^2 \vec{p}}{\partial t^2} + \vec{\nabla}\times(\vec{\nabla}\times\vec{p}) + \vec{\nabla}\frac{\partial \gamma_p}{\partial t} = -n\vec{v} + \vec{J}_b ,$$

where $\vec{J}_b$ denotes the current density of the electron bunch. Poisson's equation reads

$$-\frac{\partial}{\partial t}\vec{\nabla}\cdot\vec{p} - \vec{\nabla}^2\gamma_p = n_0 - n + \rho_b ,$$

where ρ_b is the charge density of the electron bunch.

Applying the quasistatic approximation (all fields depend on z and t only through $\zeta = z - v_\varphi t \approx z - t$) and using slab geometry, we find

$$\frac{\partial^2 p_z}{\partial x \partial \zeta} - \frac{\partial^2 \gamma_p}{\partial x \partial \zeta} = -nv_x + J_{b,x} ,$$

$$\frac{\partial^2 p_z}{\partial \zeta^2} - \frac{\partial^2 p_z}{\partial x^2} + \frac{\partial^2 p_x}{\partial x \partial \zeta} - \frac{\partial^2 \gamma_p}{\partial \zeta^2} = -nv_z + J_{b,z} ,$$

$$\frac{\partial^2 p_x}{\partial x \partial \zeta} + \frac{\partial^2 p_z}{\partial \zeta^2} - \frac{\partial^2 \gamma_p}{\partial x^2} - \frac{\partial^2 \gamma_p}{\partial \zeta^2} = n_0 - n + \rho_b .$$

Approximating the bunch current as $J_{b,x}=0$, $J_{b,z}=\rho_b=-n_b$ immediately leads to Eq. (1):

$$\frac{\partial^2\Phi}{\partial\zeta^2}-\frac{\partial^2\Phi}{\partial x^2}-\frac{\partial^2}{\partial x\partial\zeta}\left(\frac{1}{\eta}\frac{\partial^2\Phi}{\partial x\partial\zeta}\right)+\eta\Phi = \eta\gamma_p-\frac{\partial^2\gamma_p}{\partial x^2}+n_b,$$

where the wakefield potential Φ is defined as

$$\Phi=\gamma_p-p_z$$

and η is

$$\eta=\frac{n}{\gamma_p}.$$

All field variables can be expressed as functions of Φ:

$$\eta=\frac{1}{\Phi}\left(n_0+\frac{\partial^2\Phi}{\partial x^2}\right),$$

$$p_x=-\frac{1}{\eta}\frac{\partial^2\Phi}{\partial x\partial\zeta},$$

$$p_z=\frac{1}{2\Phi}(1-\Phi^2+p_x^2+2I),$$

$$\gamma_p=\frac{1}{2\Phi}(1+\Phi^2+p_x^2+2I),$$

$$E_x=\frac{\partial p_x}{\partial\zeta}-\frac{\partial\gamma_p}{\partial x},$$

$$B_y=\frac{\partial p_x}{\partial\zeta}-\frac{\partial p_z}{\partial x},$$

$$E_z=\frac{\partial p_z}{\partial\zeta}-\frac{\partial\gamma_p}{\partial\zeta}.$$

In the linear (small-amplitude) regime, η and γ_p are independent of Φ:

$$\Phi=1+\delta\Phi(|\delta\Phi|\ll 1)\rightarrow\gamma_p\approx 1+I,\quad \eta\approx n_0,$$

so that

$$\left[\left(n_0+\frac{\partial^2}{\partial\zeta^2}\right)\left(n_0-\frac{\partial^2}{\partial x^2}\right)+\frac{1}{n_0}\frac{dn_0}{dx}\frac{\partial^3}{\partial x\partial\zeta^2}\right]\delta\Phi = n_0\left(n_0-\frac{\partial^2}{\partial x^2}\right)I+n_0n_b.$$

This is the equation for linear wakefields in a plasma channel, previously derived in [13].

[1] T. Tajima and J.M. Dawson, Phys. Rev. Lett. **43**, 267 (1979).
[2] J.R. Marquès, J.P. Geindre, F. Amiranoff, P. Audebert, J.C. Gauthier, A. Antonetti, and G. Grillon, Phys. Rev. Lett. **76**, 3566 (1996).
[3] C.W. Siders, S.P. Le Blanc, D. Fisher, T. Tajima, M.C. Downer, A. Babine, A. Stepanov, and A. Sergeev, Phys. Rev. Lett. **76**, 3570 (1996).
[4] E. Esarey, P. Sprangle, J. Krall, A. Ting, and G. Joyce, Phys. Fluids B **5**, 2690 (1993).
[5] Y. Ehrlich, C. Cohen, A. Zigler, J. Krall, P. Sprangle, and E. Esarey, Phys. Rev. Lett. **77**, 4186 (1996).
[6] K. Krushelnick, A. Ting, C.I. Moore, H.R. Burris, E. Esarey, P. Sprangle, and M. Baine, Phys. Rev. Lett. **78**, 4047 (1997).
[7] C.E. Clayton, K.-C. Tzeng, D. Gordon, P. Muggli, W.B. Mori, C. Joshi, V. Malka, Z. Najmudin, A. Modena, D. Neely, and A.E. Dangor, Phys. Rev. Lett. **81**, 100 (1998).
[8] P. Sprangle, B. Hafizi, and P. Serafim, Phys. Rev. Lett. **82**, 1173 (1999).
[9] P. Sprangle, B. Hafizi, and J.R. Peñano, Phys. Rev. E **61**, 4381 (2000).
[10] E. Esarey, C.B. Schroeder, B.A. Shadwick, J.S. Wurtele, and W.P. Leemans, Phys. Rev. Lett. **84**, 3081 (2000).
[11] T.C. Chiou, T. Katsouleas, C. Decker, W.B. Mori, J.S. Wurtele, G. Shvets, and J.J. Su, Phys. Plasmas **2**, 310 (1995).
[12] C.B. Schroeder, D.H. Whittum, and J.S. Wurtele, Phys. Rev. Lett. **82**, 1177 (1999).
[13] N.E. Andreev, L.M. Gorbunov, V.I. Kirsanov, K. Nakajima, and A. Ogata, Phys. Plasmas **4**, 1145 (1997).
[14] N.E. Andreev, L.M. Gorbunov, and A.A. Frolov, Plasma Phys. Rep. **24**, 825 (1998).
[15] G. Shvets and X. Li, Phys. Plasmas **6**, 591 (1999).
[16] S.-Y. Chen, M. Krishnan, A. Maksimchuk, R. Wagner, and D. Umstadter, Phys. Plasmas **6**, 4739 (1999).
[17] C.I. Moore, K. Krushelnick, A. Ting, H.R. Burris, R.F. Hubbard, and P. Sprangle, Phys. Rev. E **61**, 788 (2000).
[18] F. Dorchies, F. Amiranoff, V. Malka, J.R. Marquès, A. Modena, D. Bernard, F. Jacquet, Ph. Miné, B. Cros, G. Matthieussent, P. Mora, A. Solodov, J. Morillo, and Z. Najmudin, Phys. Plasmas **6**, 2903 (1999).
[19] D. Umstadter, J.K. Kim, and E. Dodd, Phys. Rev. Lett. **76**, 2073 (1996).
[20] E. Esarey, R.F. Hubbard, W.P. Leemans, A. Ting, and P. Sprangle, Phys. Rev. Lett. **79**, 2682 (1997).
[21] E. Esarey, C.B. Schroeder, W.P. Leemans, and B. Hafizi, Phys. Plasmas **6**, 2262 (1999).
[22] T.C. Chiou and T. Katsouleas, Phys. Rev. Lett. **81**, 3411 (1998).
[23] A. Reitsma, R. Trines, and V. Goloviznin, IEEE Trans. Plasma Sci. (to be published).
[24] P. Kung, H.-C. Lihn, H. Wiedemann, and D. Bocek, Phys. Rev. Lett. **73**, 967 (1994).
[25] M.J. van der Wiel (private communication).
[26] T.R. Clark and H.M. Milchberg, Phys. Rev. E **61**, 1954 (2000).
[27] E. de Wispelaere, V. Malka, S. Hüller, F. Amiranoff, S. Baton,

R. Bonadio, M. Casanova, F. Dorchies, R. Haroutunian, and A. Modena, Phys. Rev. E **59**, 7110 (1999).
[28] A.G. Khachatryan, Phys. Rev. E **60**, 6210 (1999).
[29] K.V. Lotov, Phys. Plasmas **5**, 785 (1998).
[30] L.M. Gorbunov, P. Mora, and T.M. Antonsen, Jr., Phys. Rev. Lett. **76**, 2495 (1996).
[31] E. Esarey, J. Krall, and P. Sprangle, Phys. Rev. Lett. **72**, 2887 (1994).
[32] N.E. Andreev, L.M. Gorbunov, and V.I. Kirsanov, Phys. Plasmas **2**, 2573 (1995).
[33] R.D. Ruth, A.W. Chao, P.L. Morton, and P.B. Wilson, Part. Accel. **17**, 171 (1985).
[34] S.C. Wilks, T. Katsouleas, J.M. Dawson, P. Chen, and J.J. Su, IEEE Trans. Plasma Sci. **15**, 210 (1987).
[35] T. Katsouleas, S. Wilks, P. Chen, J.M. Dawson, and J.J. Su, Part. Accel. **22**, 81 (1987).
[36] T. Katsouleas, C.E. Clayton, K. Wharton, R. Kinter, T. Peters, S. Heifets, and T. Raubenheimer, in *Nonlinear and Collective Phenomena in Beam Physics, Arcidosso (Italy)*, edited by S. Chattopadhyay, M. Cornacchia, C. Pellegrini, AIP Conf. Proc. No. 395, (AIP, New York, 1996), p. 75.
[37] N.E. Andreev, S.V. Kuznetsov, and I.V. Pogorelsky, Phys. Rev. Special Topics 021301 (2000).